# Strong quantum squeezing of mechanical resonator via parametric amplification and coherent feedback

Xiang You,[1] Zongyang Li,[1] and Yongmin Li[1,2,*]

[1]*State Key Laboratory of Quantum Optics and Quantum Optics Devices, Institute of Opto-Electronics, Shanxi University, Taiyuan 030006, China*

[2]*Collaborative Innovation Center of Extreme Optics, Shanxi University, Taiyuan 030006, China*

(Received 26 July 2017; published 8 December 2017)

A scheme to achieve strong quantum squeezing of a mechanical resonator in a membrane-in-the-middle optomechanical system is developed. To this end, simultaneous linear and nonlinear coupling between the mechanical resonator and the cavity modes is applied. A two-tone driving light field, comprising unequal red-detuned and blue-detuned sidebands, helps in generating a coherent feedback force through the linear coupling with the membrane resonator. Another driving light field with its amplitude modulated at twice the mechanical frequency drives the mechanical parametric amplification through a second-order coupling with the resonator. The combined effect produces strong quantum squeezing of the mechanical state. The proposed scheme is quite robust to excess second-order coupling observed in coherent feedback operations and can suppress the fluctuations in the mechanical quadrature to far below the zero point and achieve strong squeezing (greater than 10 dB) for realistic parameters.

DOI: 10.1103/PhysRevA.96.063811

## I. INTRODUCTION

Optomechanical devices are powerful tools for ultrasensitive measurement of mass, force, displacement, and acceleration [1–6]. Optomechanics facilitates quantum information processing by aiding the development of hybrid quantum devices and helps connect different physical systems [7–9]. Moreover, it provides a new platform for conducting fundamental tests in the field of macroscopic quantum physics [10]. In recent years, quantum optomechanics has progressed significantly in various aspects [11], e.g., cooling of mechanical resonators close to the ground state [12–16], squeezing of optical fields, and entanglement between light fields and mechanical resonators in optomechanical systems [17–22].

The rapid progress in quantum optomechanics has made it possible to effectively observe quantum squeezing of motion in macroscopic mechanical resonators. Various schemes have been proposed for generating squeezed mechanical states [23–41]. With the application of mechanical parametric amplification, wherein the spring constant of the resonator is modulated at twice the mechanical frequency, squeezing of the thermal noise of a classical mechanical resonator has been achieved [23]. To surpass the conventional 3-dB limit associated with parametric squeezing (the limitation is due to the instability in mechanical systems), detuned parametric amplification combined with weak measurement [24,25] and a single-quadrature feedback scheme [26,27] have been proposed and demonstrated. Recently, strong steady-state quantum squeezing of a mechanical resonator has been demonstrated using a coherent feedback process, which involves driving the optomechanical cavity with an unequal two-tone driving field [28]. On the basis of this theoretical scheme, several studies have observed the quantum squeezing of motion in mechanical resonators, and backaction evasion measurements have been performed [29–32,42–44]. Some other mechanisms have also been investigated to achieve quantum squeezing of mechanical resonators, including the transfer of squeezed states of the optical field using optomechanical systems [33,34], exploiting the Duffing nonlinearity effect, and moderately modulating optomechanical systems [35–37].

For a membrane-in-the-middle structure (MIMS), the characteristics of dielectric membranes have been well established [45–48], and membrane resonators have been coupled with standing-wave cavity modes in a linear or nonlinear manner depending on the membrane position inside the optical cavity [49–54].

In this paper, we provide a scheme for achieving strong quantum squeezing of a mechanical resonator in a MIMS optomechanical system. The membrane is coupled linearly with a two-tone driving light field and quadratically with a modulated driving light field in a simultaneous manner by positioning the membrane resonator at a specific location inside the optical cavity. The two-tone driving provides an effective coherent feedback, surpassing the 3-dB squeezing limit [28]. In addition to parameter amplification provided by the modulated driving field, quantum squeezing of the mechanical state is further improved, thus resulting in strong mechanical squeezing. This exceeds what is achievable by using either parametric process or coherent feedback operation. Another advantage of the proposed scheme is that the excess second-order coupling due to the linear coupling of the membrane resonator with the two-tone field can be avoided [31,32,55].

The rest of this paper is organized as follows. In Sec. II, we introduce the model of the optomechanical system and derive the relevant Hamiltonian terms. In Sec. III, we calculate the steady-state values of the mechanical quadrature variance by solving the quantum master equation and investigate the effects of squeezing and purity of the mechanical states on the system parameters. In Sec. IV, we discuss the effects of excess second-order coupling on the parametric threshold and the squeezed mechanical state. Finally, the conclusions of this study are given in Sec. V.

*yongmin@sxu.edu.cn

 

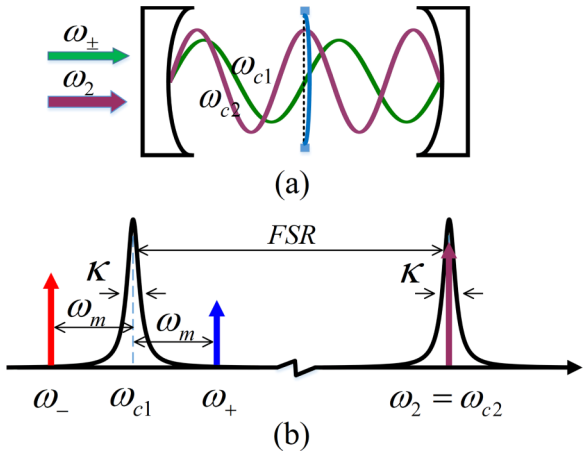


FIG. 1. (a) Schematic of the optomechanical system with two cavity modes $\omega_{c1}$ and $\omega_{c2}$, a two-tone driving field $\omega_\pm$, and a resonant driving field $\omega_2$. (b) A frequency domain representation of the cavity modes and driving field.

## II. MODEL OF OPTOMECHANICAL SYSTEM

We consider a MIMS optomechanical system, wherein two cavity modes $\omega_{c1}$ and $\omega_{c2}$ are coupled to a mechanical state via radiation pressure [Fig. 1(a)]. The driving field comprises a two-tone field $\omega_+ = \omega_{c1} + \omega_m$ and $\omega_- = \omega_{c1} - \omega_m$ and a resonant field $\omega_2 = \omega_{c2}$ [Fig. 1(b)]. Here, the field $\omega_{c2}$ is modulated at twice the mechanical frequency $\omega_m$. To meet the requirements of the specific coupling condition, the membrane is located at the center of the node and antinode of the cavity mode $\omega_{c1}$ and antinode of the cavity mode $\omega_{c2}$, simultaneously. In this scenario, the membrane couples linearly with the cavity mode $\omega_{c1}$ and quadratically with the cavity mode $\omega_{c2}$. The two cavity modes $\omega_{c1}$ and $\omega_{c2}$ are separated by a free spectral region to avoid interaction between each other.

Equations (1) and (2) show the Hamiltonian and driving Hamiltonian of the system, respectively, as follows.

$$H = \hbar\omega_{c1}a_1^\dagger a_1 + \hbar\omega_{m0}b^\dagger b + \hbar\omega_{c2}a_2^\dagger a_2 + \hbar A_1 a_1^\dagger a_1 x + \hbar A_2 a_2^\dagger a_2 x^2 + H_{dr}, \tag{1}$$

and

$$H_{dr} = i\hbar(\varepsilon_- e^{-i\omega_- t} + \varepsilon_+ e^{-i\omega_+ t})a_1^\dagger + i\hbar\varepsilon_2 e^{-i\omega_2 t} \times [1 + \lambda\sin(2\omega_m t + \theta_2)]a_2^\dagger + \text{H.c.} \tag{2}$$

Here, $a(b)$ is the photon (phonon) annihilation operator, $x = x_{zp}(b + b^\dagger)$ is the mechanical displacement operator, $x_{zp} = \sqrt{\hbar/2m\omega_m}$ is the zero-point fluctuation, $A_1 = \partial\omega_{c1}/\partial x$ is the first-order dispersion coefficient, and $A_2 = \partial^2\omega_{c2}/\partial x^2$ is the second-order nonlinear dispersion coefficient. The driving strength $|\varepsilon_i| = \sqrt{\kappa P_i/\hbar\omega_i}$ $(i = \pm, 2)$ is related to the input laser power $P_i$ and the cavity damping rate $\kappa$. $\lambda$ denotes the amplitude modulation coefficient for the resonant driving field $\omega_2$.

We apply the transformations $a_1 = \bar{\alpha}_{1,+}e^{-i\omega_+ t} + \bar{\alpha}_{1,-}e^{-i\omega_- t} + a$ and $a_2 = \bar{\alpha}_{2,0}e^{-i\omega_2 t} + (i\lambda/2)\bar{\alpha}_{2,+}e^{-i(\omega_2+2\omega_m)t - i\theta_2} - (i\lambda/2)\bar{\alpha}_{2,-}e^{-i(\omega_2-2\omega_m)t+i\theta_2} + d$ to the two cavity modes $\omega_{c1}$ and $\omega_{c2}$, respectively. Here, $\bar{\alpha}_{1,\pm} = \varepsilon_\pm/(\pm i\omega_m + \kappa/2)$ is the coherent light field amplitude of the two-tone driving laser, $\bar{\alpha}_{2,0} = \varepsilon_2/(\kappa/2)$ and $\bar{\alpha}_{2,\pm} = \varepsilon_2/(\pm i2\omega_m + \kappa/2)$ are the coherent light field amplitudes of the carrier and two sidebands of the resonant driving laser, respectively. $a$ and $d$ denote the fluctuation noises of the cavity fields $a_1$ and $a_2$, respectively. Without loss of generality, we assume $\bar{\alpha}_{1,\pm}$ and $\bar{\alpha}_{2,0}$ to be real and set $\theta_2 = \arctan(4\omega_m/\kappa)$, which guarantees that $\bar{\alpha}_2 = \bar{\alpha}_{2,\pm}e^{\mp i\theta_2}$ is also real. We transform the system to a rotating frame defined by the free Hamiltonian $H_0 = \hbar\omega_{c1}a_1^\dagger a_1 + \hbar\omega_m b^\dagger b + \hbar\omega_{c2}a_2^\dagger a_2$, where $\omega_m = \omega_{m0} + \Lambda$, $\omega_{m0}$ is the intrinsic mechanical frequency, and $\Lambda = 2A_2x_{zp}^2(|\bar{\alpha}_{2,0}|^2 + \lambda^2|\bar{\alpha}_2|^2/2)$ is the mechanical frequency shift caused by the second-order coupling. Here, we focus on the good-cavity limit $\kappa \ll \omega_m$ and apply a rotating-wave approximation. By neglecting the nonlinear terms $a$ and $d$, we can write the Hamiltonian in the interaction picture as follows.

$$H = \hbar G_-(a^\dagger b + ab^\dagger) + \hbar G_+(ab + a^\dagger b^\dagger) + i\hbar\frac{\chi}{2}(b^2 - b^{\dagger 2}) + \hbar\mu(d + d^\dagger)(b^\dagger b + bb^\dagger) + i\hbar\frac{\delta}{2}(d + d^\dagger)(b^2 - b^{\dagger 2}), \tag{3}$$

where $G_\pm = A_1x_{zp}|\bar{\alpha}_{1,\pm}|$ is the linear coupling strength, $\chi = 2A_2x_{zp}^2\lambda|\bar{\alpha}_2||\bar{\alpha}_{2,0}|$ is the second-order coupling strength due to the modulated field, and $\mu = A_2x_{zp}^2|\bar{\alpha}_{2,0}|$ and $\delta = \lambda A_2x_{zp}^2|\bar{\alpha}_2|$ are the second-order coupling strength due to the fluctuation of $a_2$. The first two terms in Eq. (3) describe the cooling process via the red-detuned driving field and heating process via the blue-detuned driving field, respectively. However, in the presence of both processes, an equivalent coherent feedback process is observed. This suppresses the fluctuation of the quadrature component $X$ below the zero-point level [28]. The third term describes a typical parametric process due to the modulated field. This can further squeeze the fluctuations in the quadrature component $X$, as shown in Sec. III. The last two terms are the second-order coupling between the fluctuation field $d$ and the membrane. The corresponding coupling strength $\mu$ and $\delta$ are considerably lower than $\Lambda$ and $\chi$, respectively. These perturbations with respect to the mechanical frequency and parametric process are negligible. Based on the above consideration, we neglected the fluctuation field $d$ and considered the cavity mode $a_2$ as a classical field. In this case, the Hamiltonian of Eq. (3) is simplified as follows.

$$H = \hbar G_-(a^\dagger b + ab^\dagger) + \hbar G_+(ab + a^\dagger b^\dagger) + i\hbar\frac{\chi}{2}(b^2 - b^{\dagger 2}). \tag{4}$$

## III. SQUEEZING OF MECHANICAL RESONATOR

### A. Quantum master equation

The dynamics of the system is described using the following quantum master equation.

$$\dot{\rho} = i[\rho, H]/\hbar + \kappa D[a]\rho + \gamma(n_{th}+1)D[b]\rho + \gamma n_{th}D[b^\dagger]\rho, \tag{5}$$

where $D[o]\rho = o\rho o^\dagger - (o^\dagger o\rho + \rho o^\dagger o)/2$, denoting the Lindblad superoperator $o$ for the damping of the cavity mode and

mechanical state. $\gamma$ is the mechanical dissipation rate, and $n_{th}$ is the number of initial thermal phonons.

We start from the Routh-Hurwitz criterion [56] and derive the stability condition of the system as follows.

$$16(G_-^2 - G_+^2) < (\kappa - 2\chi)^2. \tag{6}$$

In the following, the properties of the system are analyzed in the parameter regime where the above condition is satisfied. We introduce two motion quadratures for the mechanical resonator: $X = (b + b^\dagger)/\sqrt{2}$ and $Y = -i(b - b^\dagger)/\sqrt{2}$. Considering $\gamma \ll \kappa$, the steady-state squeezed quadrature variance $\langle X^2 \rangle$ can be determined by solving the quantum master equation.

$$\begin{aligned}\langle X^2 \rangle = & \frac{\kappa(\kappa + 2\chi) + 4(G_-^2 - G_+^2)}{2(\kappa + 2\chi)[\kappa\chi + 2(G_-^2 - G_+^2)]}\gamma n_{th} \\ & - \chi \frac{\kappa(\kappa + 2\chi) + 4(G_-^2 - G_+^2)}{2(\kappa + 2\chi)[\kappa\chi + 2(G_-^2 - G_+^2)]} \\ & - \frac{4\kappa G_+(G_- - G_+)}{2(\kappa + 2\chi)[\kappa\chi + 2(G_-^2 - G_+^2)]} + \frac{1}{2}. \end{aligned} \tag{7}$$

From Eq. (7), we find that the parametric process leads to an increase in the optical damping of the quadrature $X$. The first term describes the classical cooling process. The subsequent two terms describe the feedback forces due to the parametric process and coherent feedback operation, respectively. They together suppress the fluctuations in $X$ to be far below the zero-point level. In this scenario, we can obtain a higher squeezing level compared to the scheme wherein only a coherent feedback operation or only parametric process is employed. The last term is associated with the zero-point fluctuation.

The variance of the antisqueezing motion quadrature $Y$ is given as follows.

$$\begin{aligned}\langle Y^2 \rangle = & \frac{\kappa(\kappa - 2\chi) + 4(G_-^2 - G_+^2)}{2(\kappa - 2\chi)[-\kappa\chi + 2(G_-^2 - G_+^2)]}\gamma n_{th} \\ & + \chi \frac{\kappa(\kappa - 2\chi) + 4(G_-^2 - G_+^2)}{2(\kappa - 2\chi)[-\kappa\chi + 2(G_-^2 - G_+^2)]} \\ & + \frac{4\kappa G_+(G_- + G_+)}{2(\kappa - 2\chi)[-\kappa\chi + 2(G_-^2 - G_+^2)]} + \frac{1}{2}. \end{aligned} \tag{8}$$

The parametric amplification leads to a decrease in the optical damping of the quadrature $Y$ and destabilizes the mechanical system. Both the parametric and coherent feedback processes increase the fluctuations in the quadrature $Y$. To avoid the instability and obtain a steady-state mechanical squeezing, the drive strength of the parametric process should not exceed the threshold given by $\chi_{th} = 2(G_-^2 - G_+^2)/\kappa$.

### B. Solutions and analysis

Figure 2 shows the squeezing level of the motion quadrature variance $\langle X^2 \rangle$ as a function of the blue-tone driving strength $G_+$ (normalized by the red-tone driving strength $G_-$). If $\chi = 0$, i.e., without parametric amplification, a motion squeezing of 7.6 dB is obtained for $G_+/G_- = 0.85$. When the drive strength reaches the threshold $\chi_{th}$, the motion squeezing improves up to 3 dB on the basis of the two-tone driving and further

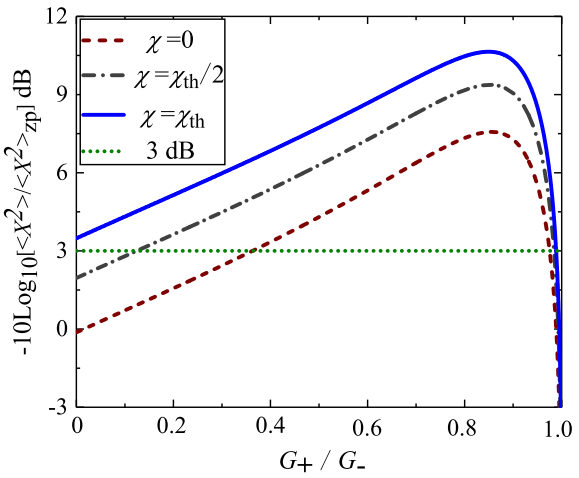


FIG. 2. Squeezing level of the motion quadrature variance $\langle X^2 \rangle$ as a function of the blue-tone driving strength $G_+$ (normalized by the red-tone driving strength $G_-$). The dotted line indicates the 3-dB squeezing limit (parameters: $n_{th} = 10^3$, $\kappa = 5 \times 10^5$ Hz, $G_- = 10^5$ Hz, and $\gamma = 1$ Hz).

increases to 10.6 dB. Note that even for a moderate drive strength, e.g., $\chi = \chi_{th}/2$, the squeezing can be enhanced by 1.8 dB. With regard to Fig. 2, the relevant experimental parameters are obtained from Ref. [15], where the occupation number of the initial thermal phonons is $n_{th} \approx 10^3$ and the mechanical frequency is $\omega_m \approx 2\pi \times 1.48$ MHz. To satisfy the good-cavity limit, the cavity parameter is modified to $\kappa \approx \omega_m/20$. The linear coupling strength satisfies $G_- \leqslant \kappa/4$ and remains constant at $G_- = 0.1$ MHz for the entire parameter region, thus ensuring the stability of the system [Eq. (6)].

We define the purity of the squeezed mechanical state as follows [28].

$$P = \langle X^2 \rangle \langle Y^2 \rangle. \tag{9}$$

Here, $P = 1/4$ indicates a completely (pure) squeezed mechanical state, and a higher value of $P$ implies that the purity of the state is poor. Figure 3 shows the purity $P$ of the squeezed mechanical state as a function of the parametric drive strength $\chi$. When the parametric process is not involved ($\chi = 0$), the purity $P$ degrades with increasing $G_+/G_-$ because of the heating process of the blue-detuned driving field. For optimal squeezing, which is observed at $G_+/G_- = 0.85$, the initial purity is close to 1/2. The purity of the state degrades with the increase in the parametric drive strength $\chi$. It is clear that the increase in $P$ is initially gradual and thereafter abrupt in the region where $\chi > \chi_{th}/2$. For reference, the following are the values of $P$ at four typical points (a–d) for $G_+/G_- = 0.85$: $P_a = 0.54$, $P_b = 0.58$, $P_c = 0.72$, and $P_d = 1.23$.

## IV. EFFECTS OF EXCESS SECOND-ORDER COUPLING

In Sec. II, we assumed that the two-tone driving field couples linearly with the membrane resonator. This assumption is proven valid in principle by positioning the membrane at exactly the center of the node and antinode of the cavity field, as shown in Fig. 4. In practice, if the membrane

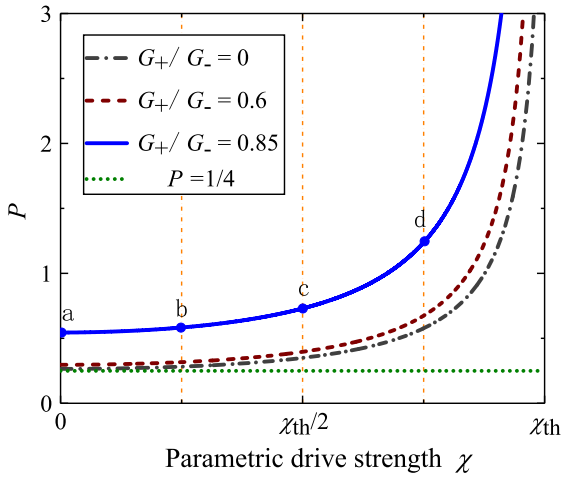


FIG. 3. Purity $P$ of the squeezed mechanical state with respect to the parametric drive strength $\chi$ for different values of $G_+/G_-$ (the values of the other parameters are the same as those shown in Fig. 2).

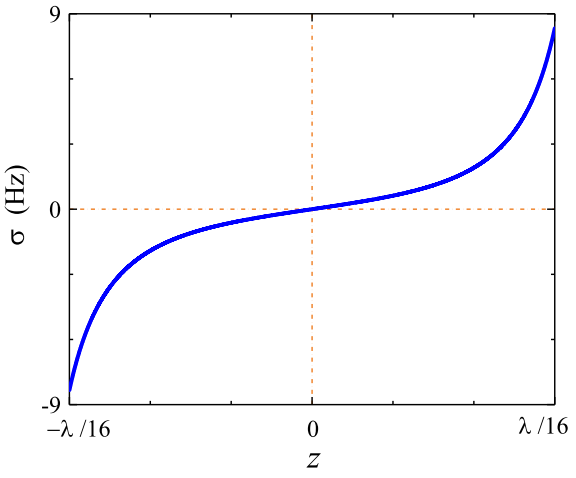


FIG. 5. Excess second-order coupling strength $\sigma$ with respect to the deviation $z$ in the membrane position (parameters: $L = 10$ mm, $\lambda = 1064$ nm, $r = 0.35$, $G_- = 0.1$ MHz, and $G_+/G_- = 0.85$).

deviates from this position, excess second-order coupling occurs, thereby inducing a heating effect and deteriorating the mechanical squeezing level. This mechanism is analyzed as follows.

The excess second-order process can be described using the second-order nonlinear dispersion coefficient $G_2 = \partial^2\omega_{c1}/\partial x^2$. In this case, an additional Hamiltonian term is introduced [31] as follows.

$$H_{ad} = \hbar\Delta b^\dagger b + \hbar\frac{\sigma}{2}(b^2 + b^{\dagger 2}), \tag{10}$$

where $\Delta = 2G_2x_{zp}^2(|\bar{\alpha}_{1,+}|^2 + |\bar{\alpha}_{1,-}|^2)$, representing the frequency shift of the mechanical resonator, and $\sigma = 2G_2x_{zp}^2|\bar{\alpha}_{1,+}||\bar{\alpha}_{1,-}|$, representing the excess second-order coupling strength. The mechanical frequency $\omega_m$ and the two-tone field frequency $\omega_\pm$ and modulated frequency $2\omega_m$ are replaced with $\tilde{\omega}_m = \omega_m + \Delta$ and $\tilde{\omega}_\pm = \omega_{c1} \pm \tilde{\omega}_m$ and $2\tilde{\omega}_m$, respectively. With the new free Hamiltonian $\tilde{H}_0 = \hbar\omega_{c1}a_1^\dagger a_1 + \hbar\tilde{\omega}_m b^\dagger b + \hbar\omega_{c2}a_2^\dagger a_2$ and by following the same procedure as before, the Hamiltonian for the interaction picture is rewritten as follows.

$$\tilde{H} = \hbar G_-(a^\dagger b + ab^\dagger) + \hbar G_+(ab + a^\dagger b^\dagger) + i\hbar\frac{\chi}{2}(b^2 - b^{\dagger 2}) + \hbar\frac{\sigma}{2}(b^2 + b^{\dagger 2}). \tag{11}$$

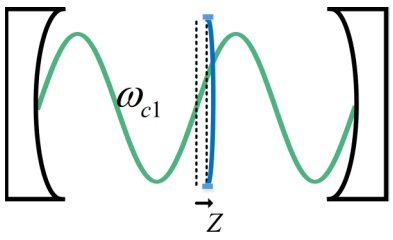


FIG. 4. Schematic of a position-detuned membrane resonator.

By combining the last two terms, Eq. (11) can be rewritten as follows.

$$\tilde{H} = \hbar G_-(a^\dagger b + ab^\dagger) + \hbar G_+(ab + a^\dagger b^\dagger) + \frac{i\hbar}{2}(\chi_1 b^2 - \chi_2 b^{\dagger 2}), \tag{12}$$

where $\chi_1 = \chi - i\sigma$ and $\chi_2 = \chi + i\sigma$. In contrast to Eq. (4), the parameter threshold decreases, i.e., $\tilde{\chi}_{th} = \sqrt{\chi_{th}^2 - \sigma^2}$, because of the excess second-order coupling.

To evaluate the strength $\sigma$, we start from the linear dispersion coefficient [48].

$$A_1 = -\frac{2r\omega_{c1}}{L}\frac{\sin(2kz)}{\sqrt{1 - r^2[\cos(2kz)]^2}}, \tag{13}$$

where $L$ is the length of the Fabry-Pérot cavity, $r$ is the amplitude reflectivity of the membrane, $k = 2\pi/\lambda$, representing the resonant wave vector; $z$ denotes the relative displacement of the membrane from the center of the node and antinode of the cavity mode $\omega_{c1}$. From Eq. (13), we can obtain the second-order dispersion coefficient as follows.

$$G_2 \approx -\frac{4kr\omega_{c1}}{L}\frac{\cos(2kz)}{\sqrt{1 - r^2[\cos(2kz)]^2}}. \tag{14}$$

Finally, we obtain the expression for $\sigma$ as follows.

$$\sigma = -2G_+G_-L\frac{\cos(2kz)\sqrt{1 - r^2[\cos(2kz)]^2}}{cr[\sin(2kz)]^2}. \tag{15}$$

Here, the constant $c$ is the speed of light in vacuum. Figure 5 shows the curve of $\sigma$ as a function of the deviation $z$, wherein a maximum displacement of $\pm\lambda/16$ is used for evaluating $\sigma$. In the entire displacement range, $\sigma$ is lower than $\pm 9$ Hz, which is considerably lower than the initial parametric threshold $\chi_{th} \approx 11$ kHz for $G_+/G_- = 0.85$. Therefore, the variation in the parameter threshold due to the excess second-order coupling is negligible.

Figure 6 shows the mechanical squeezing level with respect to the excess second-order coupling strength $\sigma$. When $\sigma = \pm 20$ Hz, the squeezing level reduces by approximately 0.06

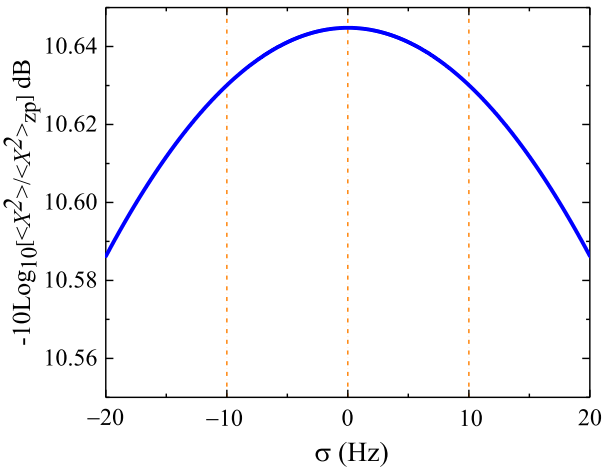


FIG. 6. Mechanical squeezing level with respect to the excess second-order coupling strength (parameters: $\chi = 11$ kHz and $G_+/G_- = 0.85$; the values of the other parameters are the same as those shown in Fig. 2).

dB. Therefore, we can conclude that the mechanical squeezing is largely immune to the excess second-order coupling and that the proposed scheme is quite robust to the deviation in the membrane position.

## V. CONCLUSION

Coherent feedback and parametric amplification were combined to achieve steady-state quantum squeezing in a MIMS optomechanical system. The scheme can suppress the fluctuations in the mechanical quadrature to far below the zero point and achieve strong squeezing (greater than 10 dB) for realistic parameters. In addition, the effects of excess second-order coupling due to the deviation in the membrane resonator position on the parameter threshold of the system and squeezed mechanical state were analyzed. The results show that the effects are negligible.

## ACKNOWLEDGMENTS

This research was supported by the National Key R&D Program of China (Project No. 2016YFA0301403), the National Natural Science Foundation of China (NSFC) (Grants No. 11774209 and No. 61378010), Shanxi 1331KSC, and the Program for the Outstanding Innovative Teams of Higher Learning Institutions of Shanxi.

[1] C. M. Caves, K. S. Thorne, R. W. P. Drever, V. D. Sandberg, and M. Zimmermann, Rev. Mod. Phys. **52**, 341 (1980).
[2] V. Peano, H. G. L. Schwefel, C. Marquardt, and F. Marquardt, Phys. Rev. Lett. **115**, 243603 (2015).
[3] D. J. Wilson, V. Sudhir, N. Piro, R. Schilling, A. Ghadimi, and T. J. Kippenberg, Nature (London, UK) **524**, 325 (2015).
[4] B.-B. Li, Q.-Y. Wang, Y.-F. Xiao, X.-F. Jiang, Y. Li, L. X. Xiao, and Q. H. Gong, Appl. Phys. Lett. **96**, 251109 (2010).
[5] J. Moser, J. Güttinger, A. Eichler, M. J. Esplandiu, D. E. Liu, M. I. Dykman, and A. Bachtold, Nat. Nanotechnol. **8**, 493 (2013).
[6] C. B. Møller, R. A. Thomas, G. Vasilakis, E. Zeuthen, Y. Tsaturyan, M. Balabas, K. Jensen, A. Schliesser, K. Hammerer, and E. S. Polzik, Nature (London, UK) **547**, 191 (2017).
[7] Y.-D. Wang and A. A. Clerk, Phys. Rev. Lett. **108**, 153603 (2012).
[8] R. W. Andrews, R. W. Peterson, T. P. Purdy, K. Cicak, R. W. Simmonds, C. A. Regal, and K. W. Lehnert, Nat. Phys. **10**, 321 (2014).
[9] S. L. Braunstein and P. V. Loock, Rev. Mod. Phys. **77**, 513 (2005).
[10] W. Marshall, C. Simon, R. Penrose, and D. Bouwmeester, Phys. Rev. Lett. **91**, 130401 (2003).
[11] M. Aspelmeyer, T. J. Kippenberg, and F. Marquardt, Rev. Mod. Phys. **86**, 1391 (2014).
[12] J. Chan, T. P. M. Alegre, A. H. Safavi-Naeini, J. T. Hill, A. Krause, S. Gröblacher, M. Aspelmeyer, and O. Painter, Nature (London, UK) **478**, 89 (2011).
[13] A. H. Safavi-Naeini, J. Chan, J. T. Hill, Thiago P. Mayer Alegre, A. Krause, and O. Painter, Phys. Rev. Lett. **108**, 033602 (2012).
[14] C. Schäfermeier, H. Kerdoncuff, U. B. Hoff, H. Fu, A. Huck, J. Bilek, G. I. Harris, W. P. Bowen, T. Gehring, and U. L. Andersen, Nat. Commun. **7**, 13628 (2016).
[15] R. W. Peterson, T. P. Purdy, N. S. Kampel, R. W. Andrews, P.-L. Yu, K. W. Lehnert, and C. A. Regal, Phys. Rev. Lett. **116**, 063601 (2016).
[16] J. D. Teufel, T. Donner, D. Li, J. W. Harlow, M. S. Allman, K. Cicak, A. J. Sirois, J. D. Whittaker, K. W. Lehnert, and R. W. Simmonds, Nature (London, UK) **475**, 359 (2011).
[17] T. P. Purdy, P.-L. Yu, R. W. Peterson, N. S. Kampel, and C. A. Regal, Phys. Rev. X **3**, 031012 (2013).
[18] A. H. Safavi-Naeini, S. Gröblacher, J. T. Hill, J. Chan, M. Aspelmeyer, and O. Painter, Nature (London, UK) **500**, 185 (2013).
[19] D. W. C. Brooks, T. Botter, S. Schreppler, T. P. Purdy, N. Brahms, and M. Stamper-Kurn, Nature (London, UK) **488**, 476 (2012).
[20] T. A. Palomaki, J. D. Teufel, R. W. Simmonds, and K. W. Lehnert, Science **342**, 710 (2013).
[21] P. Sekatski, M. Aspelmeyer, and N. Sangouard, Phys. Rev. Lett. **112**, 080502 (2014).
[22] R. Ghobadi, S. Kumar, B. Pepper, D. Bouwmeester, A. I. Lvovsky, and C. Simon, Phys. Rev. Lett. **112**, 080503 (2014).
[23] D. Rugar and P. Grütter, Phys. Rev. Lett. **67**, 699 (1991).
[24] A. Szorkovszky, A. C. Doherty, G. I. Harris, and W. P. Bowen, Phys. Rev. Lett. **107**, 213603 (2011).
[25] A. Szorkovszky, G. A. Brawley, A. C. Doherty, and W. P. Bowen, Phys. Rev. Lett. **110**, 184301 (2013).
[26] A. Vinante and P. Falferi, Phys. Rev. Lett. **111**, 207203 (2013).
[27] M. Poot, K. Y. Fong, and H. X. Tang, New J. Phys. **17**, 043056 (2015).
[28] A. Kronwald, F. Marquardt, and A. A. Clerk, Phys. Rev. A **88**, 063833 (2013).
[29] E. E. Wollman, C. U. Lei, A. J. Weinstein, J. Suh, A. Kronwald, F. Marquardt, A. A. Clerk, and K. C. Schwab, Science **349**, 952 (2015).

[30] F. Lecocq, J. B. Clark, R. W. Simmonds, J. Aumentado, and J. D. Teufel, Phys. Rev. X **5**, 041037 (2015).
[31] J.-M. Pirkkalainen, E. Damskägg, M. Brandt, F. Massel, and M. A. Sillanpää, Phys. Rev. Lett. **115**, 243601 (2015).
[32] C. U. Lei, A. J. Weinstein, J. Suh, E. E. Wollman, A. Kronwald, F. Marquardt, A. A. Clerk, and K. C. Schwab, Phys. Rev. Lett. **117**, 100801 (2016).
[33] K. Jähne, C. Genes, K. Hammerer, M. Wallquist, E. S. Polzik, and P. Zoller, Phys. Rev. A **79**, 063819 (2009).
[34] G. S. Agarwal and S. Huang, Phys. Rev. A **93**, 043844 (2016).
[35] R. Almog, S. Zaitsev, O. Shtempluck, and E. Buks, Phys. Rev. Lett. **98**, 078103 (2007).
[36] A. Mari and J. Eisert, Phys. Rev. Lett. **103**, 213603 (2009).
[37] X.-Y. Lü, J.-Q. Liao, L. Tian, and F. Nori, Phys. Rev. A **91**, 013834 (2015).
[38] M. Asjad, G. S. Agarwal, M. S. Kim, P. Tombesi, G. Di Giuseppe, and D. Vitali, Phys. Rev. A **89**, 023849 (2014).
[39] A. A. Batista, Phys. Rev. E **86**, 051107 (2012).
[40] M. G. Genoni, M. Bina, S. Olivares, G. D. Chiara, and M. Paternostro, New J. Phys. **17**, 013034 (2015).
[41] M. Rashid, T. Tufarelli, J. Bateman, J. Vovrosh, D. Hempston, M. S. Kim, and H. Ulbricht, Phys. Rev. Lett. **117**, 273601 (2016).
[42] A. A. Clerk, F. Marquadt, and K. Jacobs, New J. Phys. **10**, 095010 (2008).
[43] J. B. Hertzberg, T. Rocheleau, T. Ndukum, M. Savva, A. A. Clerk, and K. C. Schwab, Nat. Phys. **6**, 213 (2010).
[44] J. Suh, A. J. Weinstein, C. U. Lei, E. E. Wollman, S. K. Steinke, P. Meystre, A. A. Clerk, and K. C. Schwab, Science **344**, 1262 (2014).
[45] D. J. Wilson, C. A. Regal, S. B. Papp, and H. J. Kimble, Phys. Rev. Lett. **103**, 207204 (2009).
[46] J. D. Thompson, B. M. Zwickl, A. M. Jayich, F. Marquardt, S. M. Girvin, and J. G. E. Harris, Nature (London, UK) **452**, 72 (2008).
[47] C. Biancofiore, M. Karuza, M. Galassi, R. Natali, P. Tombesi, G. Di Giuseppe, and D. Vitali, Phys. Rev. A **84**, 033814 (2011).
[48] A. M. Jayich, J. C. Sankey, B. M. Zwickl, C. Yang, J. D. Thompson, S. M. Girvin, A. A. Clerk, F. Marquardt, and J. G. E. Harris, New J. Phys. **10**, 095008 (2008).
[49] A. Nunnenkamp, K. Børkje, J. G. E. Harris, and S. M. Girvin, Phys. Rev. A **82**, 021806 (2010).
[50] J. C. Sankey, C. Yang, B. M. Zwickl, A. M. Jayich, and J. G. E. Harris, Nat. Phys. **6**, 707 (2010).
[51] J. H. Teng, S. L. Wu, B. Cui, and X. X. Yi, J. Phys. B: At., Mol. Opt. Phys. **45**, 185506 (2012).
[52] M. Karuza, M. Galassi, C. Biancofiore, C. Molinelli, R. Natali, P. Tombesi, G. D. Giuseppe, and D. Vitali, J. Opt. **15**, 025704 (2013).
[53] C. Jiang, Y. Cui, and G. Chen, Sci. Rep. **6**, 35583 (2016).
[54] H. Xie, G.-W. Lin, X. Chen, Z.-H. Chen, and X.-M. Lin, Phys. Rev. A **93**, 063860 (2016).
[55] J. Suh, M. D. Shaw, H. G. Le-Duc, A. J. Weinstein, and K. C. Schwab, Nano Lett. **12**, 6260 (2012).
[56] E. X. DeJesus and C. Kaufman, Phys. Rev. A **35**, 5288 (1987).